Fracture 1977, Volume 1, ICF4, Waterloo, Canada, June 19 - 24, 1977

ASPECTS OF FRACTURE IN THE PRODUCTION AND SERVICE OF WELDED STRUCTURES

N. F. Eaton, A. G. Glover and J. T. McGrath*

ABSTRACT

This paper reviews fracture processes that take place in ferrous base materials during welding, in the immediate post-weld period and when the weldment is in service. In the welding and post-weld periods cracking due to solidification, "ductility dip" and hydrogen, as well as lamellar tearing and reheat cracking, are discussed. The service performance of weldments is dependent upon the fracture toughness of the various weld regions. The importance of microstructure in the control of fracture toughness is emphasized. The incidence of fracture in welded structures can be reduced by the proper choice of welding consumables and procedures, and through correct weld joint design.

INTRODUCTION

The principal origin of fracture in fabricated engineering structures occurs at welded joints. The welding process produces local microstructural changes that are seldom considered in the operational design analysis. The metallurgical condition of the materials is changed; local residual stresses of magnitude well beyond the component design stress may be introduced and frequently defects are produced during the joining process which go undetected. These defects, together with unfavourable design geometries provide further stress concentrations, usually in regions of metallurgically susceptible microstructures. The combined effects on fracture are often overlooked by the designer, fabricator and user of the component. Many catastrophic failures have occurred for these reasons [1].

One of the most important factors in fracture of welded components is the presence of undetected cracks. Cracks may be in regions with properties different from the base materials on which design specifications are usually based. Cracks can be introduced either during the welding operation, or during the subsequent post-welding period.

The first part of this paper outlines cracking during the fabrication stage. The second part of the paper discusses the fracture resistance of the weld metal and the heat-affected-zone, which are the main regions where fabrication-induced cracking would occur. The discussion of weld zone fracture properties is of course relevant to the performance of defect-free structures. Such an ideal state of affairs is, however, unlikely to occur in practice. Hence the fracture mechanics relationships which have evolved are highly relevant to the performance of welded joints.

*Canadian Welding Development Institute, Toronto, Ontario, Canada.

FRACTURE DURING FABRICATION

Defects that are introduced during fabrication can be divided into two main classes -- those that occur during welding and those which develop after completion of the weld and during post-weld heat treatment. The first class includes those described as solidification, liquation or ductility dip cracking [2], and lamellar tearing [3]. Cracks which develop during the post-weld period are principally hydrogen-induced cold cracking and stress relief cracking. The latter occurs mainly in post-weld stress relief heat treatment of creep resisting steels.

Fracture which occurs during welding can be further divided into two sub-classifications, depending upon the temperature of formation (Figure 1). Solidification [4] and liquation cracking [2] occur at temperatures close to the melting point. They are characterized by boundary separations associated with microsegregation, leading to the formation of lower melting point phases distributed along boundary interfaces. Ductility dip [2] cracking occurs at lower temperatures and at grain boundaries which are free from films. Lamellar tearing [3] is largely associated with decohesion of segregated non-metallic inclusions within the parent material.

Fractures after completion of welded joints involve diffusion controlled embrittlement and are time dependent. Hydrogen cracking is associated with the diffusion of hydrogen, and its influence on defects in low temperature hard transformation products at near ambient temperatures [5]. Post-weld heat treatment fracture [6] is primarily associated with precipitation mechanisms and grain boundary segregation causing exhaustion of creep ductility by cavity growth.

These fracture processes are described in more detail in the next section.

Fracture During Welding

Solidification cracking requires two necessary factors:

1. Intergranular segregation of a liquid phase which wets grain boundaries, or a solid phase which covers a larger fraction of grain boundaries greater than randomly dispersed inclusions. Such segregates are referred to loosely as "films".

2. Strain which increases as the weld pool solidifies in the area of the film until the metal grains part. The strain can be a combination of sliding and tension.

The addition of solutes such as sulphur and phosphorous to iron not only depresses the melting point but also leads to separation of the liquidus and solidus, hence establishing a freezing range. They also form low melting point compounds with iron. Solutes which are less soluble in the solid than in the liquid are rejected during solidification. The existance of a solute-rich and hence low melting point layer provides the constitutional undercooling required for the cellular or dendritic growth observed in classical solidification cracking [7]. Cracking may be located between the boundaries of the blocks of cells, grains, or dendrites [8].

Liquation cracking can occur in the heat-affected-zone (Figure 2) or the reheated region of a multipass weld. It occurs when the metal is just below the solidus of its bulk matrix. During the thermal cycle, although the bulk of the metal remains solid, some liquid pockets can form due to

the presence of sulphides, carbides and inter-metallic phases. Where liquation cracks occur in the weld metal it is confined to the reheated region; if films occur in both reheated and as-deposited regions then solidification cracking would be the more appropriate term.

Ductility dip cracking occurs at boundaries which are free from films and is generally associated with a ductility trough. It has been observed in a wide range of metals and alloys but is mainly confined to face centred cubic structures which are generally considered to have good ductility at all temperatures. However, elevated temperature tensile testing reveals that virtually all fcc materials display a ductility dip at between one-half and two-thirds of the melting point (Figure 1). In many alloys this is merely of academic interest, but in certain austenitic alloys (25 Cr - 20 Ni) the embrittlement can cause cracking during welding [9].

Examination of the fracture surfaces reveals that the cracks are intergranular and the opening of the cracks varies gradually with geometric regularity, particularly when sliding and tensile displacements are present. In many respects the intergranular separations resemble Stroh-McLean wedge cracks [10], [11] and the cavities are similar to those encountered in creep rupture [12]. Electron fractography carried out on this type of cracking shows a thermally faceted structure sometimes decorated with a small dispersion of carbides [2]. The risk of cracking is enhanced in materials with a high proof stress that increases by work hardening or precipitation because of the higher resolved shear stresses that can be induced at grain boundaries.

Lamellar tearing occurs primarily in rolled plate constructions, and is caused by thermal strains. The tearing always lies within the base plate, often outside the visible heat-affected-zone, and generally parallel to the weld fusion boundary [3]. For tearing to occur, two main conditions must be satisfied:

1. Strains must develop in the short transverse direction of the plate. These strains arise from weld metal shrinkage in the joint but can be greatly increased by strains developed from reaction with other joints in restrained structures, and the weld orientation must be such that the strains act through the joint across the plate thickness, i.e., the fusion boundary is roughly parallel to the plate surface.

2. The material must be susceptible to tearing, i.e., the plate must have poor ductility in the short transverse (through thickness) direction.

All structural steels contain inclusions, mainly of the manganese sulphide, manganese silicate and oxide types [13], arising from chemistry and deoxidation reactions. During rolling these inclusions deform into plates or discs lying parallel to the plate surface. These provide planes of weakness when the plate is stressed in the through thickness direction (Figure 3). The most important metallurgical actions that can be taken to avoid lamellar tearing, therefore, are, (a) to lower the overall inclusion content; and (b) to modify the shape of inclusion particles.

Fracture in the Post-Weld Period

The second main classification of welding defects is cracking that occurs after welding or during post-weld heat treatment.

Hydrogen cracking still remains a major problem to fabricators, particularly in low alloy or quenched and tempered constructional steels. The problem is most commonly found in heat-affected-zones, but can also occur in weld metal (Figure 4). Hydrogen can be introduced into the weldment at various stages of manufacture and service. In welding, hydrogen from moisture breakdown in the arc atmosphere is dissolved in the liquid weld metal. If the weld is cooled rapidly, considerable quantities may be retained and subsequently diffuse into the surrounding material.

A twinned martensite microstructure is most susceptible to hydrogen cracking, followed by untwinned (low carbon) martensite, lower bainite, upper bainite, and finally, mixtures of ferrite and pearlite.

Hydrogen embrittlement [14] and the associated areas of hydrogen diffusion and solubility, including interactions with defects, has received much attention [15]. The four main mechanisms postulated are:

1. *Pressure Mechanism* - postulates that hydrogen cracking is caused by recombination of the diffusing hydrogen atom to molecular hydrogen in internal voids or jogs followed by a substantial build-up of pressure.

2. *Surface Energy* - postulates that the embrittlement is caused by a reduction of surface energy by adsorbed hydrogen. Hence in a Griffith criteria, where $\sigma_f \propto \sqrt{\gamma_s}$, adsorption of hydrogen leads to an increase in brittleness.

3. *Cohesive Energy* - suggests that hydrogen influences the atomic bond breaking at the tip of a crack and hence can be related to effects on the interatomic cohesive force.

4. *Dislocation Mobility Model* - says that hydrogen influences service embrittlement by reducing the local stress required for dislocation motion, leading to solid solution softening, a lower local yield stress and hence a lower stress intensity for crack propagation.

Reheat Cracking is a form of creep rupture, and occurs principally in creep resisting steels, especially the Cr, Mo, V series. As the temperature is raised during the stress-relieving cycle, the relaxation of the residual stresses by creep processes may exhaust the creep ductility of the material in question. This inability of the grain boundaries to adsorb deformation leads to reheat cracking (Figure 5). In this case, during the stress relief thermal cycle, vanadium carbide re-precipitates within the grain interior of the coarse heat-affected-zone as fine precipitates coherent with the matrix, thus stiffening the grain interior. As a consequence, any resulting deformation is off-loaded on to the grain boundaries. If the strain applied exceeds the available grain boundary cohesive strength, failure ultimately occurs. The situation is exacerbated by impurity elements in the grain boundary which prevent sliding and act as sites for nucleation of the cavities [16], [17].

In susceptible materials, initiation probably takes place during heating. Acoustic emission [17], [18] has shown many events in the 500°-690°C temperature range. A peak of emission at a particular temperature was followed by relative quiet, the length of the quiet period depending on the material and stress range. Often there was only a short time between periods of activity. The frequency of peaks increased during testing, with very high activity prior to failure.

For a range of Cr, Mo, V steels it has been shown by Myers [19] that no measureable deformation occurs until a temperature of about 600°C is reached, i.e., in the temperature region in which the first significant peaks are detected. Failure occurs later with as little as 1% deformation. Cavities in these steels nucleate at grain boundary particles, probably carbides, when grain boundary shear takes place. This occurs when the temperature is high enough to permit creep deformation to take place. Shear is unlikely to be entirely smooth in coarse grained heat-affected-zone material and some local bursts probably occur. It is these more violent bursts of sliding which are the more likely to initiate large and stable void nuclei and with which the largest release of elastic energy must be associated. The acoustic emission peaks, therefore, are most probably generated by these more violent void nucleating activities. During the quiet periods less violent grain boundary shear takes place. Although stable voids are nucleated, their nucleation is not detected against the background. Cavity formation occurs either randomly along a grain boundary or in clusters on grain boundary facets or triple points. However, nucleation along grain facets tends to predominate, with initiation occurring preferentially along boundaries oriented at high angles to the principal stress. The final sequence of coalescence and disappearance of cavities by surface self-diffusion is shown in Figures 6 and 7, and is the same as found previously for high temperature service failures [20].

FRACTURE IN SERVICE

The fracture of a weldment in service occurs through crack initiation and subsequent propagation in a defect-free region, or from pre-existing welding defects of the type described earlier. The susceptibility to crack initiation and propagation is strongly dependent on the fracture toughness of the weldment regions. Metallurgical structure of these regions is of prime importance in controlling fracture toughness.

Weld Metal Toughness

Weld metal fracture toughness of C/Mn and micro alloy steels will be considered in terms of resistance to cleavage and ductile fracture.

(a) *Microstructural Features* - When weld metal solidifies and cools the microstructure may be composed of a mixture of transformation products, including proeutectoid ferrite, coarse and fine bainite, and martensite. The type and amount of transformation product depends upon weld metal composition and cooling rate.

Another transformation product, termed acicular ferrite, has been reported principally in weldments of low carbon (< 0.1%) micro alloy steels [21]. This structure is difficult to distinguish from fine bainite which forms at a lower transformation temperature. Examples of the various transformation products are illustrated in Figure 8.

A zone of refined grains is found within multipass weld metal. The refined zone forms when the temperature from subsequent weld passes exceeds the Ac_3 temperature.

Non-metallic inclusions are also a feature of weld metal microstructure. Inclusions are oxide and silicate particles which are generally spherical in shape, Figure 8d. The volume fraction of inclusions in the weld metal is dependent upon the slag-metal reactions which take place during welding.

The resistance to cleavage failure in weld metal is dependent upon the type and amount of certain transformation products, while inclusions influence the resistance to ductile fracture.

(b) *Resistance to Cleavage Failure* - Because of the mixture of transformation products in a weld deposit it is a complex task to define the ideal structure for optimum fracture toughness or resistance to cleavage failure. The use of quantitative metallography [22] allows one to relate the type and amount of weld metal microconstituents to fracture resistance.

Several investigations [22], [23], [24] of weld metal in C/Mn and micro alloy steels have revealed that a high volume fraction of coarse proeutectoid ferrite, coarse upper bainite and lath (untwinned) martensite are detrimental to toughness, while fine bainite structure with a low volume fraction of fine carbide particles is conducive to high toughness properties. This is illustrated in Table I, which relates Charpy transition temperature to weld metal microstructure. The control of weld microstructure, and thus fracture toughness, is attained through control of weld composition and cooling rate.

It is appropriate to review the role of weld metal composition. The principal alloying elements in C/Mn steel weld metal are Si, Mn, Mo, Cr and Ni. In the micro alloy steel weldments the effects of Nb, Ti and V must be examined. Because of the fairly rapid cooling rates encountered in weld processes most of the alloying elements, including the strong carbide formers such as Nb, Ti and V are likely to be retained in solid solution in the as-deposited weld.

The work of Dorschu and Stout [25] was one of the first investigations to assess the effect of individual alloying elements on the fracture toughness of single-pass submerged arc weld metal in a C/Mn A201 base metal. In Figure 9, alloy additions such as Si, Cr, Mn and Ni either have no effect or slightly improve toughness at low concentrations. However, as the amount of these elements is increased a decline in toughness can result. C and V had a detrimental effect on toughness even at relatively low level additions. Although the analysis of microstructure was limited, a refinement of the ferrite grains (proeutectoid or bainitic in nature was not made definite) was associated with increased toughness. A decrease in toughness was related to the formation of coarse bainite and an increasing proportion of carbide aggregates.

Recent studies, particularly in micro alloy steel weldments, have been more extensive in their evaluation of microstructural changes brought about by alloying elements in the weld metal. Most of the attention has been focused on high heat input welds where the dilution of Nb in the weld metal can approach 60%. The data of Sawhill [26] and Hannerz [27], Figure 10, indicate an increase in Charpy transition temperature with increasing Nb content in the weld metal. Sawhill reported that for a fixed cooling rate the weld metal microstructure changed from fine to coarse bainite as the Nb level increased to 0.05%. The increase in coarse bainite was related to the deterioration in toughness. The individual additions of Ti [28] and V [29] to weld metal may cause a similar decrease in toughness. In all of the investigations there is little information on how micro alloy additions affect the kinetics of the austenite transformation.

In order to rectify the loss in toughness attributed to micro alloy additions other elements have been added to the weld metal. For example,

Sawhill [30] increased the toughness of a weld metal containing 0.05% Nb through additions of V, Ti, Cr and Mo, made individually and in combination. This improvement in toughness was related to the refinement of the bainitic microstructure.

To attain optimum resistance to cleavage fracture it is necessary to know more about the kinetics of the transformation of austenite to lower temperature transformation products. There is a lack of continuous cooling transformation diagrams for weld metal compositions, particularly for micro alloy steel weldments. Such information would allow a welding engineer to choose the welding consumables and procedure that would result in a weld composition and cooling rate to achieve the desirable transformation products.

(c) *Resistance to Ductile Fracture* - The energy required for ductile failure of weld metal is directly related to the volume fraction, V_f, of inclusion particles, where

$$V_f \propto \frac{C}{h}$$

(C = particle size and h = interparticle spacing). This energy can be expressed as the upper shelf energy associated with the Charpy impact test or the plateau value of COD in a COD vs. temperature diagram.

The failure mechanism [31] is one of void formation by the decohesion of the inclusion particle/matrix interface followed by the plastic deformation and shear failure of the interparticle region.

Because weld metal inclusions are mainly oxides and silicates, inclusion volume fraction can be directly related to oxygen content. Taylor and Farrar [32] have compiled data on the relationship between Charpy upper shelf energy and oxygen content in submerged arc weld metal. As shown in Figure 11, shelf energy decreases with increasing oxygen content with the greatest change taking place between 300 to 600 ppm oxygen.

The control of inclusion or oxygen content in weld metal relates to the slag/metal reactions which take place during welding. The components of the flux which constitute the molten slag are oxides such as MnO, SiO_2, CaO, MgO, Al_2O_3, TiO_2 and fluorides like CaF_2. Of the above-mentioned oxides all, with the exception of SiO_2 and MnO, are stable having high standard free energies of formation [33]. SiO_2 and MnO in the molten slag can be reduced by iron if one considers near equilibrium conditions in effect and the following reaction taking place:

$$MxOy + Fe \rightleftharpoons xM + yFeO$$

where M = Si, Mn.

The reduction of SiO_2 is the principal source of oxygen in the weld metal. Whether SiO_2 in the slag can be reduced depends upon its activity. The key to controlling oxygen content in the weld metal is in reducing the activity of SiO_2 in the slag. Basic oxide components of the flux, such as CaO, can accomplish this reduction in activity by reacting with SiO_2 to form the inactive orthosilicate, $CaOSiO_2$.

There is considerable controversy [34] regarding the rating of fluxes as to their ability to reduce the activity of SiO_2 and thus lower the amount

of oxygen entering the weld metal. Whether a flux is classified by the basicity formula [35] or the ionic theory approach [36], there is a need for more thermodynamic studies of the reactions which take place in controlling the oxygen and thus the inclusion content of weld metal.

Heat-Affected-Zone (HAZ) Toughness

The factors affecting fracture toughness of the HAZ in weldments of C/Mn and micro alloy steels will be reviewed primarily with respect to resistance to cleavage failure. Less emphasis will be placed on resistance to ductile fracture because inclusion particle formation in the HAZ is not as extensive as it can be in the weld zone.

(a) *HAZ Regions* - The temperature gradient produced in the HAZ of a weldment results in a range of microstructure. The HAZ can be divided into four regions, extending outward from the weld zone - (1) the grain coarsened region (where the peak temperature, Tp $\gg$ Ac_3 temperature); (2) the grain refined region (Tp just above Ac_3 temperature); (3) intercritical region (Ac_3 > Tp > Ac_1); and (4) sub-critical region (Tp < Ac_1). The microstructure that can develop within each region depends upon such factors as peak temperature, plate composition and cooling rate. Cooling rate is usually expressed as the time required for the temperature to drop from 800° to 500°C. The magnitude of the cooling rate is determined by heat input, section thickness, geometry and preheat.

In the following discussion of HAZ fracture toughness emphasis will be given to the grain coarsened region which is potentially the most embrittled region of the HAZ.

(b) *Resistance to Cleavage Failure* - The fracture toughness of the grain coarsened region of the HAZ is controlled by microstructure. As with weld metal toughness, microconstituents such as coarse bainite and martensite are detrimental, while improved toughness is associated with a fine ferrite or fine bainitic structure. A coarse prior austenite grain size contributes to low HAZ toughness.

To illustrate the HAZ toughness in C/Mn steel weldments, various investigations can be cited [37], [38], [39], and [40]. The fracture mechanics data in Table 2 indicate that generally there was not a large difference in toughness between the HAZ and base metal for weldments 1, 2 and 3. The composition of the base metal of these weldments was nominally 0.14-0.16% C, 0.8-1.2% Mn. Although quantitative metallographic analysis was lacking, it was stated that the HAZ microstructure included proeutectoid ferrite, pearlite, together with coarse and fine bainite. However, a much larger difference in toughness between the HAZ and base material can result in a C/Mn weldment (weldment 4) when the martensite content of the HAZ increases. Generally, low heat input, i.e., < 1kJ/mm and a steel with sufficient hardenability are the factors which promote the formation of HAZ martensite.

The coarse grained HAZ of micro alloy steel weldments can exhibit a much lower fracture toughness than the base material. To account for this difference in toughness between HAZ and base material let us first examine the structural changes that can take place in the HAZ during welding. The base material has fine grains of ferrite (d = 0.01 mm) produced by a controlled rolled process. NbC and VC particles play an important role in controlling grain growth. The resultant fine grained structure has high strength and resistance to cleavage fracture. When these structures are subjected to a high heat input in the HAZ immediately adjacent to the weld

zone, the second phase particles controlling grain size may dissolve with the Nb and V going into solution. Upon cooling of the HAZ, various transformation products can form, depending on cooling rate. If cooling is rapid enough to retain alloying elements such as Nb, V in solution, these elements can have a strong influence on the type of transformation products which may result. If cooling is sufficiently slow, precipitation of Nb and V carbonitrides may take place.

Let us examine some of the studies which have been carried out to relate HAZ microstructure to toughness in micro alloy steels. The work of Cane and Dolby [37], Banks [38] and Sawhill and Wada [40] have established that Nb ($\sim$ 0.046 - 0.10%) promotes a brittle coarse bainite in the HAZ coarse grain region. Weldments 5 and 6 in Table 2 exhibit a significant difference in toughness between base metal and HAZ. The base metal composition of these weldments was nominally 0.16-0.18% C, 1.2% Mn, 0.2-0.3% Si and 0.04-0.06% Nb. These investigations suggested that the presence of Nb in solution promoted the formation of the bainitic microstructure. There was no evidence that second phase Nb carbonitrides had formed during the transformation from austenite.

Similar to the effect of Nb, increasing V content can cause a deterioration in toughness in the HAZ (Figure 12). The work of Hannerz and Jonsson-Holmquist [41] suggests that the decrease in toughness is associated with the precipitation of vanadium nitrides. This was in evidence primarily at slow cooling rates, Δt (800°-500° C) $\approx$ 300 s.

The problem of restricting HAZ grain growth in micro alloy steel weldments has been studied by Taniguchi et al [42]. When the fine, carbonitrides dissolve during high heat input welding processes, extensive grain growth can take place in the HAZ, leading to poor fracture toughness. In weld simulation tests, it was found that a steel, containing 0.14% C, 0.28% Si, 1.22% Mn with 0.014% TiN particles of a size 0.1 μm was able to maintain an austenite grain size of 50 μm at a peak temperature of 1400° C (Figure 13). The TiN particles were stable enough to restrict grain growth at the high temperatures. The transformation upon cooling from peak temperature resulted in a fine grained ferrite/pearlite microstructure. This contrasted with a coarse bainite HAZ microstructure in steel without TiN and subjected to similar thermal treatment. HAZ from actual welds in the Ti bearing steel prepared by the submerged arc and electrogas processes showed significant improvement in Charpy impact energy over conventional steel (25° C improvement in transition temperature).

In order to control HAZ toughness, more information must be obtained about the microstructural content of the HAZ. In this regard quantitative optical metallography is useful in identifying the type and amount of microconstituents. For micro alloy steel weldments, in particular, the effect of Nb and V on microstructure must be established. The use of TEM should be able to identify whether these elements are present in solution or as fine carbonitrides.

Test Specimen Selection

If useful fracture toughness data is to be obtained from steel weldments, the selection of a test specimen, particularly with respect to the notch or fatigue crack location is important. Dolby and Archer [43] have provided a selection of fracture initiation test specimens which simulate the orientation of various welding defects in the HAZ. For example, the specimen 'A' in Figure 14 simulated the orientation of a hydrogen-induced

toe crack with the notch tip sited in the HAZ.

The proximity of neighbouring regions may play a role in determining fracture toughness of the HAZ. This will greatly depend upon the plastic zone size at the notch tip. This can be illustrated by specimen 'B' in Figure 14, which can be used to simulate a crack transverse to the fusion zone. In testing a weldment of HY80 steel [44], specimen 'B' was employed with the notch positioned in two ways, (a) through the weld metal to the HAZ; and (b) through the base metal to the HAZ. A lower fracture toughness was obtained for the specimen with the notch tip adjacent to the weld metal. The plastic zone size at the tip of the notch was large enough to extend into the weld metal. Since the weld metal was low in toughness this had sufficient effect to reduce the HAZ toughness value.

With regard to weld metal toughness, Dawes [45] has reviewed the selection of fracture mechanics specimens for multipass, two-pass and single-pass butt welds. Because multipass welds contain both as-deposited and refined structures, the root of the notch should sample both weld metal regions. With reference to specimen 'A' in Figure 14 the notch should be positioned in the weld zone with the line of the notch being perpendicular to the plate surfaces. Similarly, with two-pass and single-pass butt welds a test specimen with a through thickness notch in the weld zone is recommended.

RELATIONSHIP TO FAILURES IN WELDED STRUCTURES

Many examples could be cited to show that all the defects described in the first part of the paper have resulted in premature and often catastrophic failures. These could have been avoided if suitable precautions, particularly at the fabrication stage, had been taken in the light of an understanding of the mechanisms of defect formation.

Certain defects, notably solidification cracking and lamellar tearing, require closer control of material composition, principally with respect to reducing impurity content. Often, however, such problems arise during the welding operation and the fabricator has no opportunity to instigate changes in the material or the consumables that he is using. However, much more could be done at the fabrication stage to overcome these problems by attention to welding procedure variables. For instance, solidification cracking, depending as it does on the solidification mechanisms in the weld pool, can be overcome by changes in welding current and travel speed to modify the weld metal solidification structure. Changes in weld joint design are also valuable in overcoming lamellar tearing, even in very susceptible high inclusion content steels, by ensuring shrinkage stresses are not applied in the plate through thickness direction. Hydrogen cracking can be overcome by using consumables with low hydrogen potential and attention to optimum drying and storage prior to use. Adequate preheat of the joint to assist hydrogen diffusion or influence cooling rate to produce less hardened microstructures is also an effective safeguard.

In the discussion of component fracture one of the prime objects must be to ensure that the assumptions made are not optimistic. A thorough understanding of a structure's design and operational details, together with the material properties, is required to predict likely modes of subcritical crack growth and their significance. In practice slow crack growth can occur by any one or combinations of fatigue, creep and creep-fatigue cracking, cracking by monotonic loading (ductile tearing or micro-brittle cracking).

The area of least data is the stress field surrounding the defect. Stress analysis at regions of complex geometry is difficult to do analytically and numerical computation using finite element representation of the actual design can often be used successfully. These aspects are discussed in a related plenary paper by Soete and Salkin [46].

In the area of fracture resistance, current research has identified the way ahead. In terms of resistance to cleavage and ductile fracture a much greater understanding is now available on the influence of metallurgical structure and particularly inclusions on fracture toughness. Control of metallurgical structure in weld metals and heat-affected-zones can be achieved by variations in welding conditions, such as heat input and cooling rate, but this subject has not been adequately investigated to date. Inclusion control has been widely adopted in steelmaking, particularly for improved fracture toughness in high strength micro alloy steels. Similar developments related to inclusion control in weld metals should be undertaken.

CRACK GROWTH FROM DEFECTS UNDER CREEP CONDITIONS

To ensure the integrity of welded components at high temperatures, it is necessary to be able to predict the rates of crack propagation from existing defects when cracking is caused by creep. Various approaches have been used for the analysis of creep crack growth data involving either fracture mechanics or a more generalized approach. One of the limitations of using a fracture mechanics approach is that many materials when tested under conditions producing high ductility creep deformation are "notch insensitive". This situation has been studied in many instances using standard analyses available for creeping structures. The major problems are to identify the deformation mode and stress index relevant to particular component operation and the test conditions. These problems have been overcome more recently by using a reference stress [47], or skeletal point stress [48].

However, much of the early work on Cr, Mo, V, [49] showed a good correlation between creep crack growth rate and the stress intensity parameter, K, as defined by,

$$\frac{da}{dt} = CK^n$$

where

$$\frac{da}{dt}$$

is the crack growth rate, C and n are material, temperature dependent constants; and

$$K = Y\sigma\sqrt{a}$$

where Y is a function of geometry, f(a,W), σ is the gross section stress, W is the specimen width, and a is the crack length.

Similar relationships have been found for austenitic steel [50] and for more conventional creep ductile ferritic materials [51].

While this method gives a good description for these materials, it would not be expected to hold generally, since creep is, by definition, a time dependent deformation process and elastic theory should not, in principle, be wholly applicable. This approach, however, is capable of describing the bulk of published data within less than two orders of magnitude of crack growth rate, and this is typical of scatter in creep data.

In order to overcome the problems of using a linear elastic approach two other analyses have been proposed. The first alternative has used the COD technique where crack growth is controlled by local displacements at the crack tip [52]. This is very attractive in principle since it is easily visualized [53] as deformation and fracture of a small tensile specimen at the crack tip, and for creep processes the accumulation of strain is an accepted physical picture. However, in practice this approach is difficult to apply due to inherent problems of defining a critical COD value, large experimental scatter at elevated temperatures, and the requirement of a detailed mathematical analysis to derive the total displacement relationship for any real structural defect.

The second alternative has utilized available creep rupture data and the net section stress as the controlling parameter [54]. In a study of crack growth data for normalized and tempered Cr, Mo, V at 565° C, [49] it was shown that a better correlation was obtained with net section stress than with stress intensity factor.

It is difficult to reconcile all the various crack growth models in terms of creep mechanisms because of the inherent differences in ductility shown by creeping materials. These differences in mechanisms imply differences in the distribution and accumulation of creep damage in the various materials. Hence, any crack growth analysis presented for general application should be able to account for true intercrystalline failure under conditions of time dependent deformation and the more ductile crack growth mechanism.

AVOIDANCE OF FAILURES

From the foregoing discussion it will be apparent that there is a considerable understanding of the mechanisms which cause welding defects, and of the factors that influence the fracture of structures in the weld region. Many weld fabrication problems and service failures could be avoided if this information was communicated to, and used by, the fabricators, designers and production welding engineers. As pointed out by one of the authors in a recent paper [55], there have been numerous metallurgical researches undertaken as a result of problems in welding and failures in welded structures, resulting in increased understanding of the scientific principles involved - but seldom avoiding a recurrence of the problem.

The main recommendation to achieve the goal of avoidance of failures is to ensure that information gained by research does not lie dormant on library shelves, but appears in the revision of standards and specifications or in the production manuals of the alloy-producing metallurgist or industrial welding engineer. We should ensure that what has already been learned by research is communicated to and applied in industrial practice.

REFERENCES

1. WECK, R., Met. Prog., 109, 1976, 26.
2. HEMSWORTH, B., BONISZEWSKI, T. and EATON, N. F., Met. Const. and Brit. Weld. Journal, 1, 1969, 5.
3. FARRAR, J. C. M., CHARLES, J. A. and DOLBY, R. E., Effect of Second Phase Particles on Mech. Prop. Steel, The Iron and Steel Inst., 1971, 171.
4. WOLSTENHOLME, D. A., Welding Research Related to Power Plant Conf., CEGB, 1972, 310.
5. GRAVILLE, B. A., The Principles of Cold Cracking Control in Welds, Dominion Bridge Co. Ltd., 1975.
6. MURRAY, J. D., Brit. Weld. Journal, 14, 1967, 447.
7. CHITTY, A. and BROWN, J. M., Welding Research Related to Power Plant Conf., CEGB, 1972, 293.
8. WOLSTENHOLME, D. A., Welding and Metal Fab., 40, 1972, 59.
9. HADDRILL, D. M. and BAKER, R. G., British Welding Journal, 12, 1965, 411.
10. STROH, A. N., Proc. Roy. Soc., 218, 1953, 391.
11. McLEAN, D., J. Inst. Met., 81, 1952, 293.
12. PERRY, A. J., Journal Mats. Sc., 9, 1974, 1016.
13. LITTLE, J. H. and HENDERSON, W. J. M., Effect of Second Phase Particles on the Mechanical Properties of Steel, The Iron and Steel Inst. Conf., 1971, 182.
14. SAVAGE, W. F., ASM Meeting on Sulphide Inclusions in Steel, Port Chester, N. Y., November 1974.
15. HIRTH, J. P. and JOHNSON, H. H., Corrosion, 32, 1976, 1.
16. MYERS, J., Welding Research Related to Power Plant Conf., CEGB, 1972, 356.
17. GLOVER, A. G., Conf. Applied Fracture Investigations, Munich, 1975.
18. GLOVER, A. G., HOLT, J. and WILLIAMS, J. A., Schallemission Conf., Munich, 1974.
19. MYERS, J., Weld Thermal Simulations for Research and Problem Solving, Brit. Weld. Inst. Seminar, 1972.
20. BURNS, D., JAMES, D. W. and JONES, H., Met. Sc. Journal, 7, 1973, 204.
21. GRAY, J. M., WRC Bulletin No. 213, 1976, 1.
22. WIDGERY, D. J., Welding Journal, 55, 1976, 57-s.
23. GLOVER, A. G., McGRATH, J. T. and EATON, N. F., Proc. of Conf. Materials Engineering in the Arctic, Gray Rocks, Quebec, 1976.
24. GARLAND, J. G. and KIRKWOOD, P. R., Met. Const., 7, 1975, 275, 320.
25. DORSCHU, K. E. and STOUT, R. D., Welding Journal, 40, 1961, 97-s.
26. SAWHILL, J. M., Climax Molybdenum Co. Report, L-176-115, 1973.
27. HANNERZ, N. E., VALLAND, G. and ESTERLING, K., IIW Report IX-798-72, 1972.
28. BONISZEWSKI, T., Met. Const. and Brit. Weld. Journal, 1, 1969, 225.
29. HANNERZ, N. E. and JONSSON-HOLMQUIST, B. M., Met. Const. and Brit. Weld. Journal, 6, 1974, 64.
30. SAWHILL, J. M., Climax Molybdenum Co. Report, L-176-128, 1974.
31. CHIN, L. L. J., Welding Journal, 48, 1969, 290-s.
32. TAYLOR, L. G. and FARRAR, R. A., Welding and Met. Fab., 43, 1975, 305.
33. RICHARDSON, F. D. and JEFFES, J. H. E., J. Iron and Steel Inst., 160, 1948, 261.
34. PALM, J. H., Welding and Met. Fab., 44, 1976, 135.
35. TULIANI, S. S., BONISZEWSKI, T. and EATON, N. F., Welding and Met. Fab., 37, 1969, 327.
36. ZEKE, J., Welding Research Related to Power Plant Conf., CEGB, 1972, 247.

37. CANE, M. W. F., and DOLBY, R. E., The Toughness of Weld Heat-Affected-Zones, Brit. Welding Inst., 1974, 93.
38. BANKS, E. E., Australian Welding Journal, 18, 1974, 59.
39. SAUNDERS, G. G., The Toughness of Weld Heat-Affected-Zones, Brit. Welding Inst., 1974, 32.
40. SAWHILL, J. M. and WADA, T., Welding Journal, 54, 1975, 1-s.
41. HANNERZ, N. E. and JONSSON-HOLMQUIST, B. M., Metal Science Journal, 8, 1974, 228.
42. TANIGUCHI, N., YAMATO, K., NAKASHIMA, A., MINANI, K. and KANAZAWA, S., Proc. Jap. U. S. Sem. Significance Defects in Welded Structures, 1973, 397.
43. DOLBY, R. E. and ARCHER, G. L., Proc. of Conf. on Appl. of Frac. Mech. to Pressure Vessel Tech., Instn. Mech. Eng., 1971, 190.
44. DAWES, M. G., Met. Const. and Brit. Weld. Journal, 2, 1970, 533.
45. DAWES, M. G., Welding Institute Research Bulletin, 15, 1974, 157.
46. SOETE, W., Fracture 1977, ed. D. M. R. Taplin, University of Waterloo Press, 1977, Vol. I.
47. ANDERSON, R. G., GARDNER, L. R. T. and HODGKINS, W. R., J. Mech. Eng. Sci., 5, 1963, 238.
48. MACKENZIE, A. C., Int. J. Mech. Sci., 10, 1968, 441.
49. NEATE, G. J. and SIVERNS, M. J., Conf. on Creep and Fatigue in Elevated Temperature Applications, 1973, Philadelphia.
50. JAMES, L. A., Int. J. Frac. Mech., 8, 1972, 347.
51. THORNTON, D. V., GEC (Whetstone) Report CML(1972)-18.
52. WELLS, A. A. and McBRIDE, F. H., Can. Metal Quat., 6, 1967, 347.
53. COTTRELL, A. H., Structural Processes in Creep, Iron and Steel Institute, London, 1961.
54. HARRISON, C. B. and SANDOR, G. N., Eng. Fracture Mech., 3, 1971, 403.
55. EATON, N. F., Engineering Journal, 59, 1976, 62.

Table 1 Effect of Weld Metal Microstructure on Toughness [23]

Weld	Proeutectoid Ferrite %	Fine Bainite %	Upper Bainite %	Others %	Transition Temperature °C, 68 J
1	13	76	10	1	-48
2	1	5	91	3	27
3	4	-	96	-	27
4	38	43	15	4	-32
5	1	98	1	1	-60

Table 2 HAZ and Base Plate Fracture Toughness

Weld	Weld Procedure	Heat Input kJ/mm	Weldment Region	*Tc °C
1 (37)	Sub. arc, 2 wire bead on plate	7	base HAZ	-120 -100
2 (38)	Sub. arc, 1 wire multipass butt weld	5.4	base HAZ	- 45 - 40
3 (39)	Sub. arc, 1 wire bead on plate	1	base HAZ	-120 -110
4 (39)	Sub. arc, 1 wire bead on plate	1	base HAZ	-170 - 60
5 (37)	Sub. arc, 2 wire bead on plate	5	base HAZ	-150 - 80
6 (38)	Sub. arc, 1 wire multipass butt weld	2.1	base HAZ	$\ll$ - 70 - 40

* Temperature at Critical COD of 0.1 mm

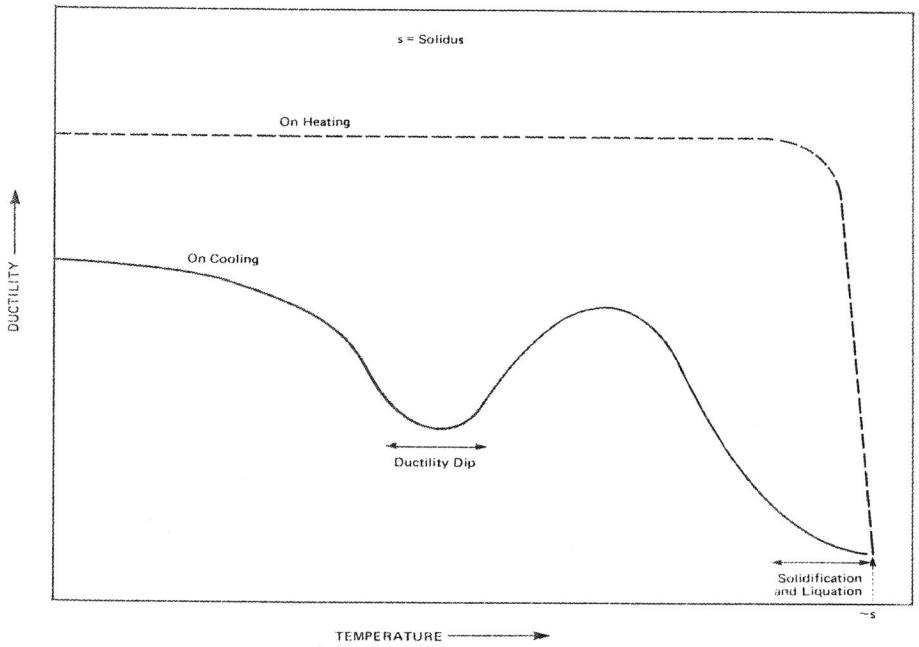

Figure 1 Schematic of the Occurrence of Solidification and Ductility Dip Cracking

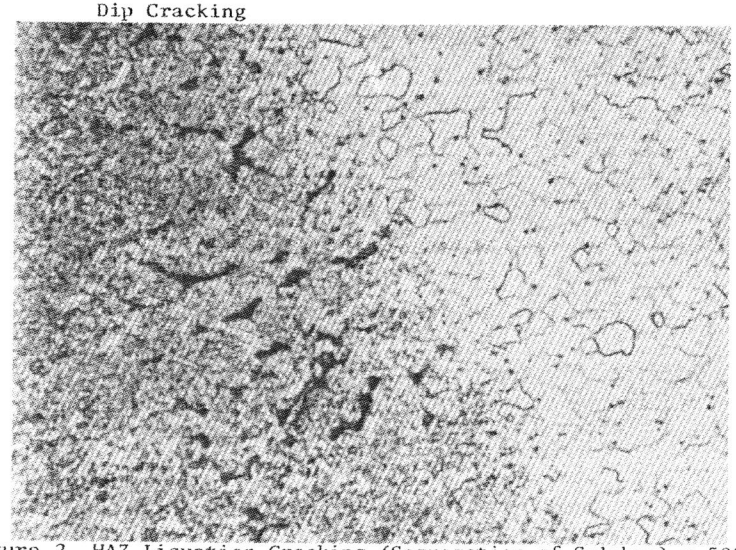

Figure 2 HAZ Liquation Cracking (Segregation of Sulphur) x 500

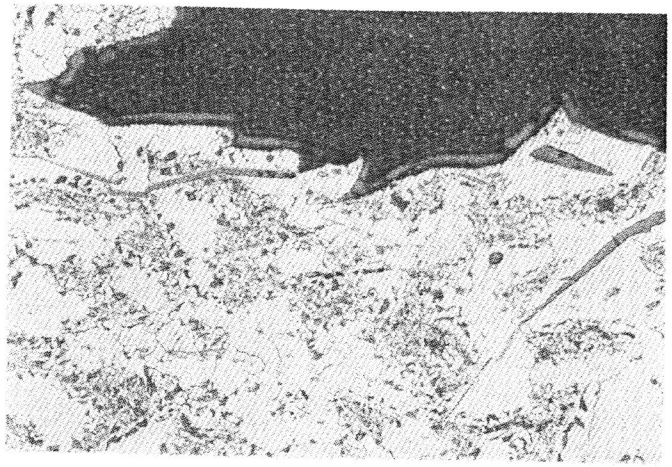

Figure 3 Elongated Maganese Sulphide Inclusions on Surface of Lamellar Tear x 200

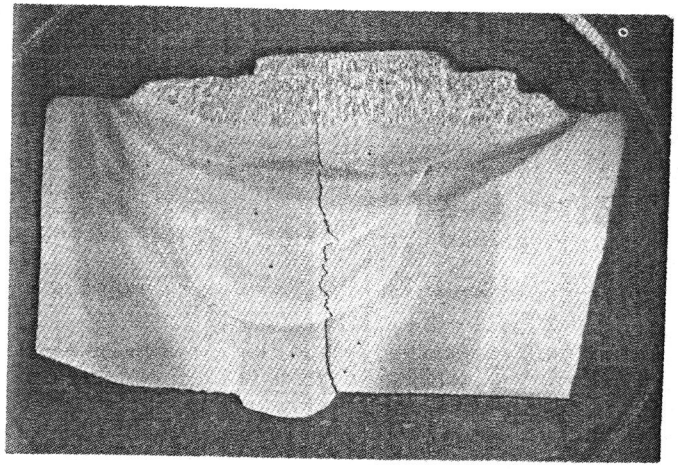

Figure 4 Hydrogen Cracking in Weld Metal x 4

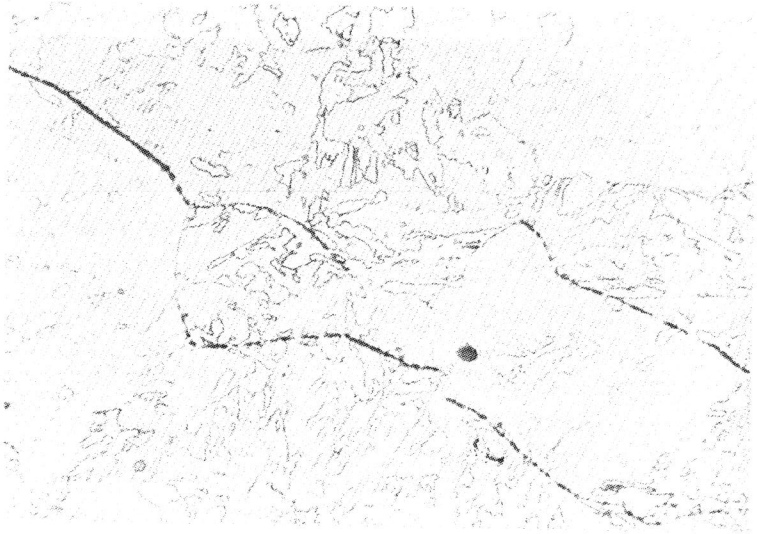

Figure 5 Cavitational Damage in Coarse Grained HAZ x 500

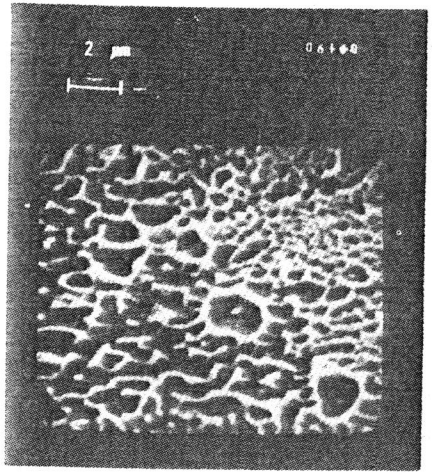

Figure 6 Fracture Face of Reheat Crack x 4000

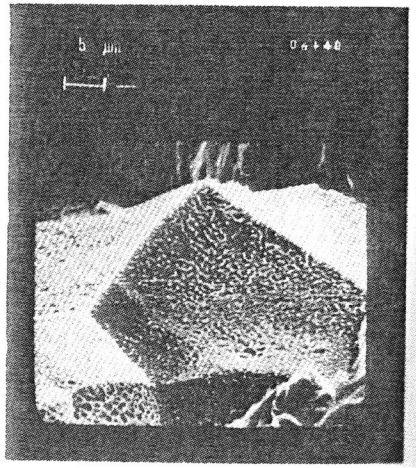

Figure 7 Smoothed Cavitated Surface x 1600

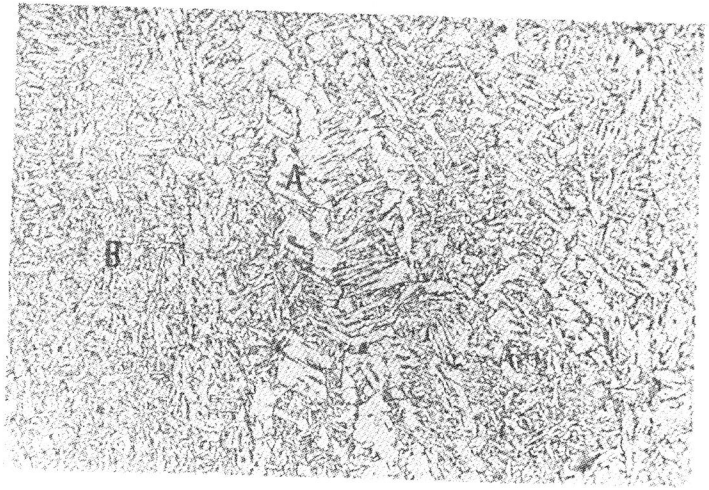

Figure 8(a) Formation of Proeutectoid Ferrite 'A' and Fine Bainite 'B' in C/Mn Steel Weld Metal x 500

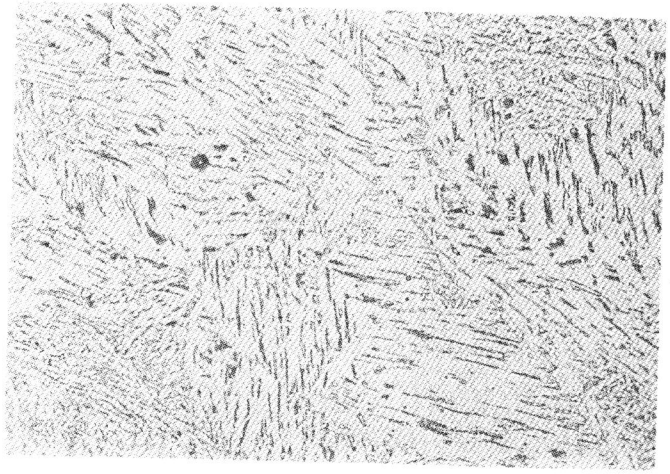

Figure 8(b) Coarse Bainite Microstructure in C/Mn Steel Weld Metal x 500

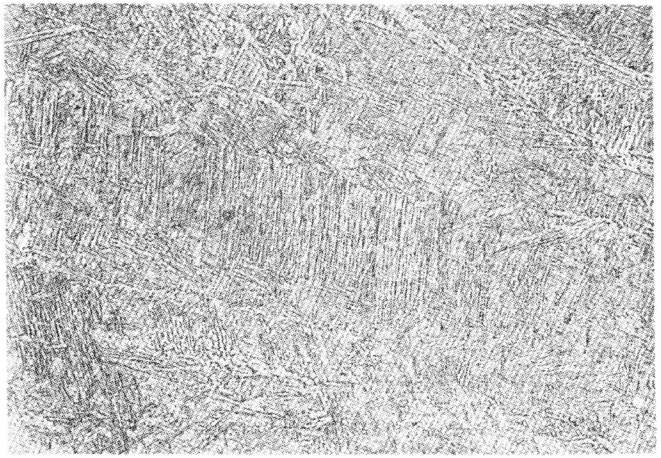

Figure 8(c) Martensitic Weld Metal Structure x 500

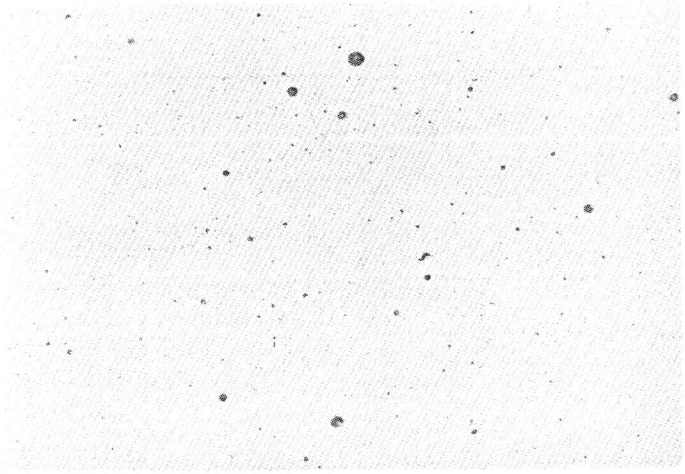

Figure 8(d) Inclusion Particles in C/Mn Steel Weld Metal x 500

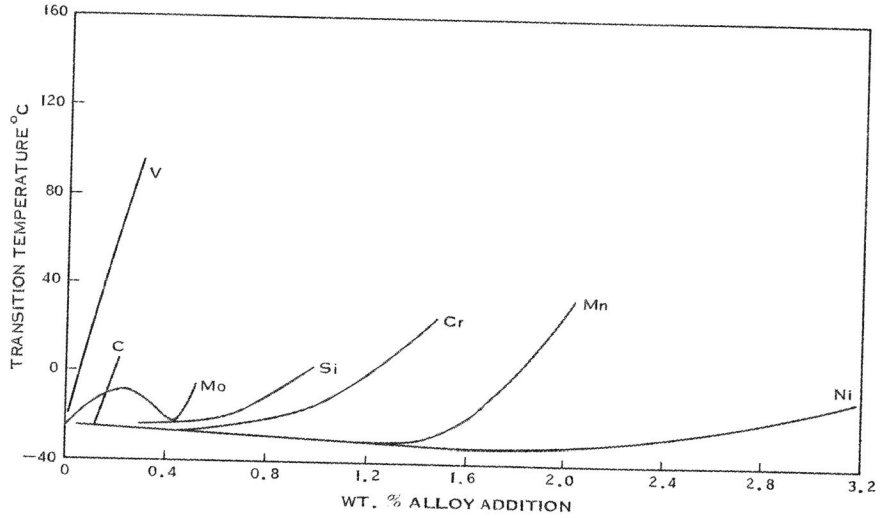

Figure 9 Effect of Alloying Elements on the Charpy Transition Temperature of Submerged Arc Weld Metal [25]

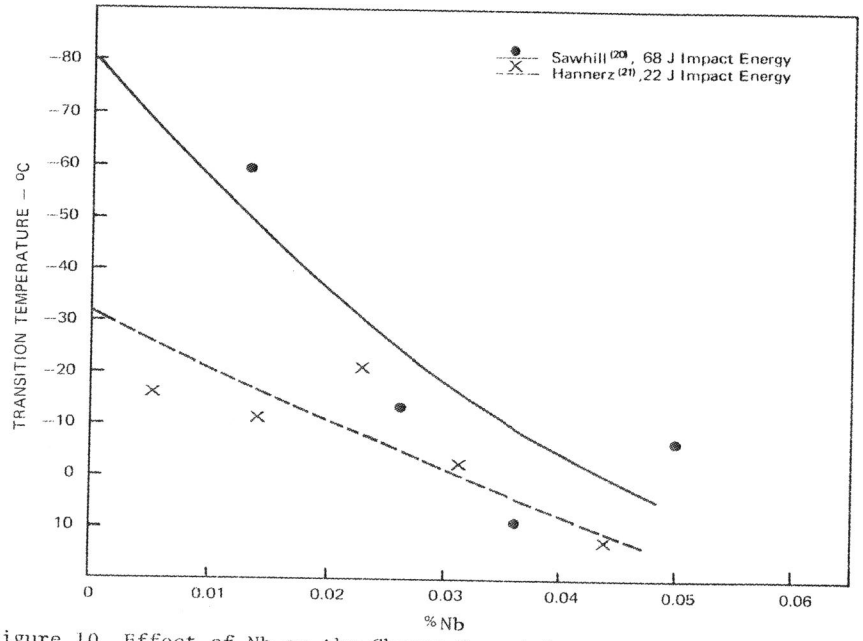

Figure 10 Effect of Nb on the Charpy Transition Temperature

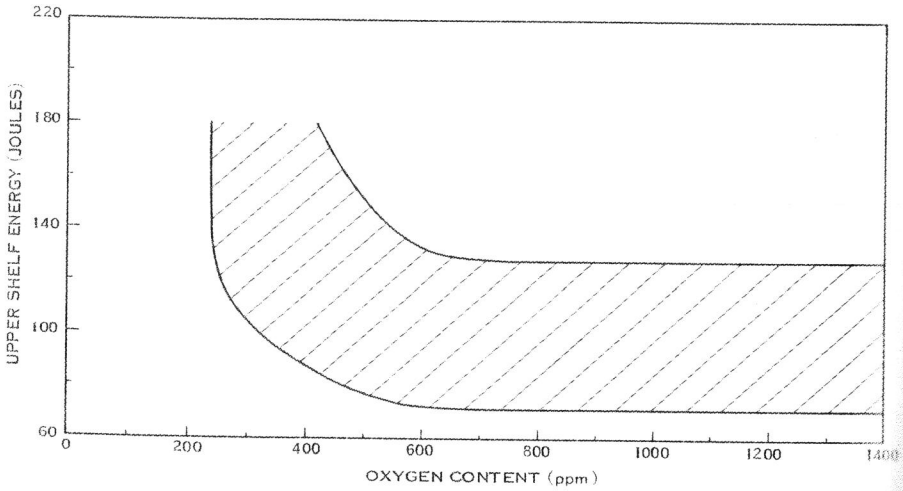

Figure 11 Effect of Weld Metal Oxygen Content on Charpy Shelf Energy [32]

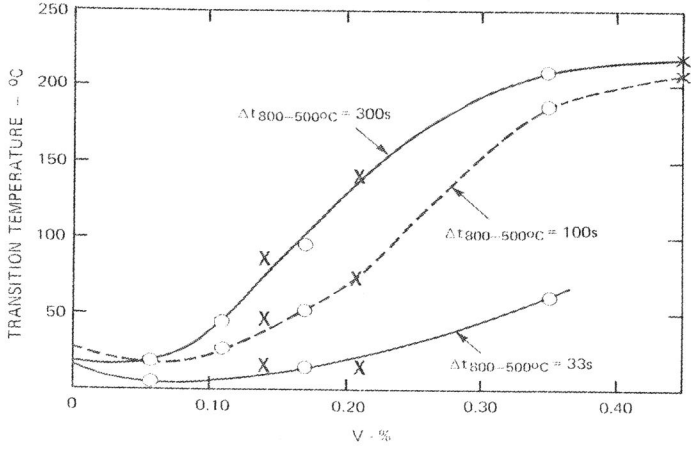

Figure 12 Effect of V on the HAZ Charpy Transition Temperature [41]

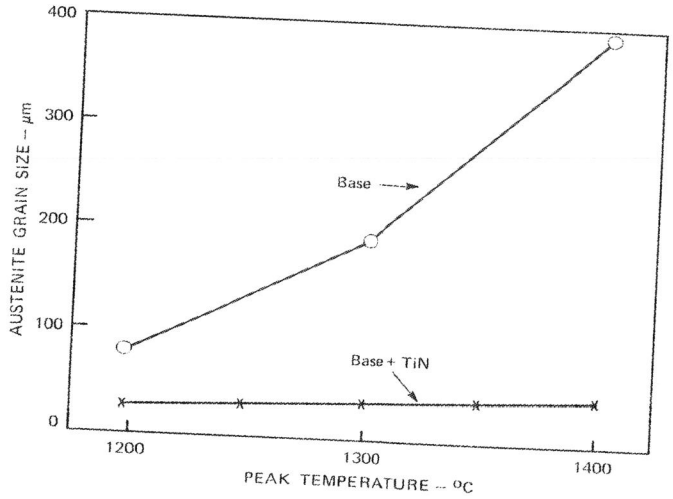

Figure 13 Relation Between Austenite Grain Size and Peak Temperature for Steels with and without TiN Particles [42]

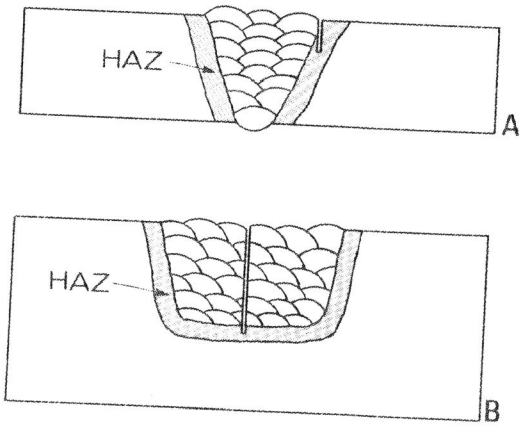

Figure 14 HAZ Fracture Toughness Test Specimens